

Unraveling Trends in Schistosomiasis: Deep Learning Insights into National Control Programs in China

Qing Su^{1,2,3}, Cici Xi Chen Bauer⁴, Robert Bergquist⁵, Zhiguo Cao⁶, Fenghua Gao⁶, Zhijie Zhang^{1,2,7,*}, Yi Hu^{1,2,7,*}

¹ Department of Epidemiology and Biostatistics, School of Public Health, Fudan University, Shanghai 200032, China

² Key Laboratory of Public Health Safety, Ministry of Education, Shanghai 200032, China

³ Xuhui District Center for Disease Control and Prevention, Shanghai 200032, China

⁴ Department of Biostatistics and Data Science, University of Texas Health Science Center at Houston, 1200 Pressler Street, Houston, TX 77030, USA

⁵ Ingerod, Brastad, Sweden

⁶ Anhui Institute of Parasitic Diseases, Wuhu, People's Republic of China 230061, China

⁷ Laboratory for Spatial Analysis and Modeling, School of Public Health, Fudan University, Shanghai 200032, China

* Corresponding author: Yi Hu (huyi@fudan.edu.cn); Zhijie Zhang (epistat@gmail.com)

Running title: Unraveling Schistosomiasis Trends by Deep Learning

1 **Abstract**

2 **Background:** To achieve the ambitious goal of eliminating schistosome infections, the Chinese
3 government has implemented diverse control strategies. This study explored the progress of the
4 2 most recent national schistosomiasis control programs in an endemic area along the Yangtze
5 River in China.

6 **Methods:** We obtained village-level parasitological data from cross-sectional surveys
7 combined with environmental data in Anhui Province, China from 1997 to 2015. A
8 convolutional neural network (CNN) based on a hierarchical integro-difference equation (IDE)
9 framework (i.e., CNN-IDE) was used to model spatio-temporal variations in schistosomiasis.
10 Two traditional models were also constructed for comparison with 2 evaluation indicators: the
11 mean-squared prediction error (MSPE) and continuous ranked probability score (CRPS).

12 **Results:** The CNN-IDE model was the optimal model, with the lowest overall average MSPE
13 of 0.04 and the CRPS of 0.19. From 1997 to 2011, the prevalence exhibited a notable trend: it
14 increased steadily until peaking at 1.6 per 1000 in 2005, then gradually declined, stabilizing at
15 a lower rate of approximately 0.6 per 1000 in 2006, and approaching zero by 2011. During this
16 period, noticeable geographic disparities in schistosomiasis prevalence were observed; high-
17 risk areas were initially dispersed, followed by contraction. Predictions for the period 2012 to
18 2015 demonstrated a consistent and uniform decrease.

19 **Conclusions:** The proposed CNN-IDE model captured the intricate and evolving dynamics of
20 schistosomiasis prevalence, offering a promising alternative for future risk modeling of the
21 disease. The comprehensive strategy is expected to help diminish schistosomiasis infection,
22 emphasizing the necessity to continue implementing this strategy.

23

24 **Key words:** deep learning; schistosomiasis; spatio-temporal model; national schistosomiasis
25 control programs

26

27 **Introduction**

28 Schistosomiasis is a chronic parasitic disease associated with poverty, caused by blood flukes
29 belonging to the genus *Schistosoma* [1, 2]. Considered by the World Health Organization as a
30 neglected tropical disease, schistosomiasis is mainly prevalent in low-resource tropical and

31 subtropical areas, with an estimated 140 million cases worldwide in 2019 [3]. Three species of
32 *Schistosoma* are commonly seen in Asia, with *Schistosoma japonicum* the most prevalent,
33 followed by *S. mekongi* and *S. malayensis* [4]. *S. japonicum* has a history of more than 2200
34 years in China [5]. Over the past 60 years, China has made significant strides in reducing the
35 prevalence of schistosomiasis; currently, fewer than 29,000 people nationwide are estimated to
36 be living with the disease, and only 5 new cases were reported in 2020 [6]. However, the risk
37 of *S. japonicum* infection still exists in some areas of China, and the goal of eliminating the
38 infection by 2030 remains a challenge [7].

39

40 Over the past 6 decades, China has made great strides toward reducing the prevalence of
41 schistosomiasis. The World Bank Loan Project (WBLP) for schistosomiasis control and
42 prevention from 1992 to 2001 made substantial progress; however, it focused on the treatment
43 (e.g., praziquantel chemotherapy) [8] and not the transmission sources (e.g., intermediate snail
44 host), and the epidemic rebounded following the end of the project. The integrated control
45 strategy implemented in 2005, which focused on eliminating the intermediate snail host, again
46 reduced the number of *S. japonicum* infections [9, 10], and the prevalence of schistosomiasis
47 in the country has now stabilized at a historical low.

48

49 In order to better understand the transmission patterns and the temporal trend of schistosomiasis,
50 previous studies employed numerous spatio-temporal models to estimate the infection risk and
51 the contributing factors. Most studies have used Kriging [11, 12], regression techniques [13,
52 14], or linear dynamic models (e.g., integro-difference equations [IDE]) [15]. However, the
53 dynamic transmission patterns of schistosomiasis are not fully captured by descriptive or linear
54 models due to the complexity of the process and the multitude of contributing factors, which
55 include environmental changes, human behavior, and evolving interventions. Therefore, in this
56 study, we have adopted a deep learning (DL) approach with the aim of capturing the intricate
57 and dynamic patterns of the disease. Our analysis provides detailed information on the annual
58 prevalence of schistosomiasis across a grid of 1×1 km. This information is valuable for both
59 researchers and local policymakers, enabling them to comprehend the evolution of

60 schistosomiasis distribution patterns under the 2 national schistosomiasis control programs
61 (NSCPs) and to identify areas in urgent need of disease intervention.

62

63 **Materials and Methods**

64 **Study area**

65 The study was conducted at the village level in Anhui Province, located in eastern China, where
66 the Yangtze River traverses the province (Figure 1). Anhui Province covers a geographic area
67 of approximately 140,100 km² and had a population of nearly 65 million in 2019
68 (<http://tjj.ah.gov.cn/>). The province experiences a humid subtropical climate, with average
69 annual temperatures ranging from 15°C to 16°C. Summers are typically hot, with temperatures
70 frequently exceeding 30°C, while winters are cooler, with temperatures often falling below
71 10°C. The region receives a significant amount of rainfall, averaging between 1,000 and 1,500
72 mm annually, with the heaviest precipitation occurring in late spring and early summer.
73 Humidity levels are generally high, often surpassing 80% during the rainy season. These
74 climatic conditions—high temperatures, ample rainfall, and elevated humidity—create an ideal
75 environment for the proliferation of *Oncomelania hupensis*, the freshwater snail that serves as
76 the intermediate host for *S. japonicum*. Therefore, snail populations increase during the warmer
77 and wetter months, which in turn affects the transmission dynamics of schistosomiasis in Anhui
78 Province.

79

80

Figure 1 about here

81

82 **Parasitological data**

83 Prevalence data for schistosomiasis from 1997 to 2015 were obtained from cross-sectional
84 surveys conducted by the Anhui Institute of Parasitic Diseases. In China, schistosomiasis is
85 classified as a Class B notifiable infectious disease, ensuring that case detection at the village
86 level is comprehensive, with a coverage rate of 100%. Upon identifying a schistosomiasis case,
87 healthcare providers are required to complete an infectious disease report card within 24 hours
88 of diagnosis for network reporting. Data collection occurred annually at the village level,
89 targeting the population aged 5-65. A 2-tiered diagnostic approach was employed: all

90 participants were initially screened using the indirect hemagglutination assay [16], and
91 positive readings were confirmed by Kato-Katz stool examinations [17] of all seropositive
92 individuals. Individuals testing positive by both methods were diagnosed with *S. japonicum*
93 infection. The study's annual selection of sample villages was systematically conducted in
94 accordance with the "Control and Elimination of Schistosomiasis (GB15976 - 1995)"
95 guidelines established by the National Health Commission of the People's Republic of China in
96 1995. Each year, villages categorized as level 1, with a human prevalence exceeding 5% in the
97 previous year, were included in the study. In contrast, villages categorized as level 2, with a
98 human prevalence below 5% in the previous year, were included every 2 years. Furthermore,
99 villages categorized as level 3, indicating a human prevalence of less than 1% in the year before,
100 were selected every 3 years. To ensure the accuracy of our disease prevalence calculations and
101 maintain consistency with the methodologies of our previous studies [12, 18], sample villages
102 with fewer than 100 participants were omitted to mitigate the impact of statistical outliers.
103 Throughout the duration of the study, the number of sample villages varied between 1028 and
104 1683. Detailed enumerations are provided in the Supplementary Material (Table S1).

105

106 **Environmental data**

107 Considering the environmental factors that affect snail habitats and the growth and reproduction
108 of *O. hupensis*, the intermedia host snail of *S. japonicum*, we included the following covariates:
109 precipitation, hours of daylight, distance to water bodies, daytime land surface temperature
110 (LST_{day}) and the normalized difference vegetation index (NDVI). We collected raster variable
111 data for the corresponding years (1997-2015) for the areas included in the study, and the data
112 for the distance to water bodies were from 2015. Average daily precipitation and hours of
113 daylight were obtained from the China Meteorological Data Sharing Service System
114 (<http://cdc.cma.gov.cn/home.do>), from 610 weather stations across China. We performed
115 Kriging interpolation to produce continuous overlays each year during the study period for all
116 of China and then extracted the interpolated meteorological measures for Anhui Province using
117 ArcGIS 10.5 (ESRI, Redlands, CA, USA). Water-body data were downloaded from the World
118 Wildlife Fund's Conservation Science Data Sets (<http://worldwildlife.org>), and the Euclidean

119 distances between the geographic centroids of each sampled villages and water bodies were
120 calculated. The NDVI and LST_{day} data were obtained from NASA's Level 1 and Atmosphere
121 Archive and Distribution System (<http://ladsweb.nascom.nasa.gov>), which included 8-day 1-
122 km² images for LST_{day} and the monthly 1-km² for NDVI. All the above data were processed
123 using annual data and the raster data with a resolution of 1 km. The detailed sources of all the
124 environmental data, as well as the resolution of time and space, are presented in the
125 Supplementary Material (Table S2).

126

127 **Statistical analysis**

128 We treated the prevalence of schistosomiasis as a continuous variable and converted it to a
129 Gaussian distribution, and the prevalence was transformed by the Box-Cox method [19] to
130 satisfy the assumptions of a Gaussian model. We used univariate analysis for initial variable
131 screening, and retained any variables with a p-value <0.1 [20]. We then assessed the correlations
132 among the remaining variables, where correlation coefficients >0.6 indicated strong
133 collinearity [21]. The 5 covariates we selected proved not to be colinear.

134

135 **Convolutional neural network (CNN)**

136 To evaluate the potential nonlinear spatio-temporal trends of schistosomiasis and the influence
137 of environmental factors, we considered a convolutional neural network (CNN) based on an
138 IDE framework (i.e., CNN-IDE) [22] to model the nonlinear trend. We employed a 2-level
139 hierarchical structure [23] in the IDE model, with a data level and a process level. The former
140 modeled the data generating mechanism, conditioned on the underlying spatial-temporal
141 process and parameters, while the latter considered the unobserved process given by the
142 parameters. Details on this CNN-IDE model can be found in the Supplementary Material.

143

144 **Model comparison and validation**

145 In addition to the CNN-IDE, we also implemented 2 spatio-temporal models (IDE and ST
146 Kriging [7]) to estimate the risk of *S. japonicum* infection. The IDE model was the same as the
147 IDE framework in CNN-IDE. Similarly, we constructed a hierarchical structure including a data

148 level and a process level. Detailed descriptions of the 2 models can be found in the
149 Supplementary Material.

150

151 Cross-validation is used to evaluate model predictions by splitting the data into training and
152 validation samples, then training the model with the training sample, and evaluating the model
153 with the validation sample. In K-fold cross-validation, the available data are randomly divided
154 into K folds. Each fold is excluded, the model is trained on the remaining K-1 folds, and then
155 the model is evaluated on the initially excluded fold. Specifically, for $k = 1, \dots, K$ folds, the model
156 is fit after removing the Kth fold, and the prediction result $\widehat{Z}_v^{(-k)}$ is obtained for $i=1 \dots m_k$,
157 where m_k is the number of data in the Kth fold. We conducted 10-fold cross-validation [23]
158 in to evaluate the performance of the 3 models and to identify the optimal model. We used 2
159 evaluation indicators, the mean-squared prediction error (MSPE) and continuous ranked
160 probability score (CRPS), which are defined as follows:

$$161 \quad MSPE = \frac{1}{Tm} \sum_{j=1}^T \sum_i^m \{Z_v(s_i; t_j) - \widehat{Z}_v(s_i; t_j)\}^2 \quad (4)$$

162 $\{Z_v(s_i; t_j)\}$ represent observations of a randomly selected 10% of samples, and $\widehat{Z}_v(s_i; t_j)$ are
163 predictions from modeling the rest of the observations.

$$164 \quad CRPS = \int (1\{Z_v \leq \widehat{Z}_v\} - F(\widehat{Z}_v))^2 d\widehat{Z}_v \quad (5)$$

165 Where $1\{Z_v \leq \widehat{Z}_v\}$ indicates that if Z_v is less than x , the value is 1, otherwise 0, and $F()$ is
166 the cumulative distribution function of the observed 10% of samples. Smaller values of MSPE
167 and CRPS indicate better model performance. Our analyses were all done in R (version 3.6.3,
168 R Foundation for Statistical Computing, Vienna, Austria; <http://cran.r-project.org>). A high-
169 resolution spatial prediction (1 km²) of schistosomiasis prevalence was mapped using the
170 optimal model.

171

172 **Results**

173 As shown in Figure 2, the median annual prevalence of schistosomiasis began to increase in
174 1997 and reached a peak in 2005 (1.6 per 1000). There was a sharp decline to 0.6 per 1000 in
175 2006, and the prevalence continued to decrease rapidly, approaching zero after 2010. The mean

176 annual prevalence exhibited a similar pattern. The interquartile range widened from 0-0.8 (per
 177 1000) in 1997 to 1.2-2.4 (per 1000) in 2005, then diminished to 0% by 2013.

178

179 **Figure 2 about here**

180

181 Figure 3 presents the results of model comparison. As shown in the figure, both the MSPE and
 182 CRPS for the CNN-IDE model were lower than those from the other 2 models for most of years.
 183 The overall average MSPE values of the CNN-IDE model, the IDE model, and ST Kriging
 184 model were 0.04, 0.05 and 0.06, respectively, and the overall CRPS values were 0.19, 0.22 and
 185 0.25, respectively.

186

187 **Figure 3 about here**

188

189 Table 1 shows the final environmental covariates and parameters in the CNN-IDE model. The
 190 average daily precipitation ($p=0.02$) and NDVI ($p <0.01$) showed statistically significant
 191 positive associations with schistosomiasis prevalence, while LST_{day} ($p <0.01$), with longer
 192 hours of daylight ($p <0.01$), and distance to a water body ($p <0.01$) exhibited statistically
 193 significant negative associations. The estimate for the diffusion parameter $\theta_{p,1}$ was $2.31E+02$,
 194 and those for the shift parameters $\theta_{p,2}$, and $\theta_{p,3}$ were $6.50E-03$ and $2.45E-02$, respectively.

195

196 **Table 1. Estimations of parameters for schistosomiasis in the CNN-IDE model.**

Parameters	Estimate	Standard error	<i>z</i>	<i>p</i>
Intercept	-2.76	1.23	-7.78	<0.01
Average daily precipitation	1.35E-05	1.63	2.26	0.02
Hours of daylight	-1.13E-03	0.42	-10.21	<0.01
Distance to water body	-8.44E-03	0.19	6.61	<0.01
LST_{day}	-1.17E-05	1.12	-7.24	<0.01
NDVI	4.16E-06	0.10	-6.71	<0.01
$\theta_{p,1}^a$	2.31E+02	10.11	1.89	0.21
$\theta_{p,2}^b$	6.50E-03	13.01	2.01	0.14

$\theta_{p,3}^d$ 2.45E-02 10.92 3.92 0.04

197 CNN, convolutional neural network; IDE, integro-difference equation; LST_{day} , daytime land
198 surface temperature; NDVI, normalized difference vegetation index.

199 ^aDiffusion parameter.

200 ^bShift parameter.

201

202 A map of the annual predicted prevalence for schistosomiasis is displayed in Figure 4. Starting
203 in 1997, the prevalence was relatively high and showed a gradual increase, as indicated by the
204 expanding yellow areas and the occasional red spots. The epidemic reached its peak in 2005,
205 characterized by extensive light yellow and small red areas. Following this peak, the prevalence
206 began to decline and remained relatively stable at a low level from 2006 to 2011. The
207 predictions, represented by a dark green shade, showed a consistent uniformity across the study
208 area, with values nearing zero from 2012 to 2015. Figure 5 illustrates the standard error of the
209 corresponding estimates, indicating that the values were higher in areas where the sample
210 villages were less densely distributed. However, the standard errors remained low throughout
211 the study period.

212

213

Figures 4 and 5 about here

214 **Discussion**

215 Our study presents a comprehensive application of advanced DL methods for quantifying local
216 trends of schistosomiasis prevalence to assess the effectiveness of 2 NSCPs in the Yangtze River
217 Basin, China. These estimates highlight substantial differences within the study area in levels
218 and trends. The annual predicted prevalence map illustrates the disease's progression, showing
219 fluctuating trends until a relatively stable low level after 2011. These findings contribute to our
220 understanding of schistosomiasis dynamics and control strategies currently implemented in
221 China.

222

223 The environmental factors that affect snail habitats and the growth and reproduction of the
224 snails have been confirmed in previous studies [12, 24-26]. A study found that an ideal snail
225 habitat is distributed less than 1 km from the water source [24]. In line with this, our study

226 found a negative association between the proximity to water bodies and the prevalence of
227 schistosomiasis. Increased rainfall can facilitate the dispersal of snails to new areas, including
228 rivers, lakes, and wetlands [4]. The optimal survival temperature for the eggs of the parasite
229 varies between 16°C and 35°C [27], a fact that supports the transmission of *S. japonicum* in
230 snails that reproduce and grow under conditions of higher LST_{day} and therefore longer hours of
231 daylight. Vegetation could reduce solar radiation and regulate the water temperature for host
232 snails, thus providing comfortable spawning shelters [25]. As a result, a higher NDVI is more
233 conducive to snail survival.

234

235 The results of model comparison indicated that our CNN-IDE was the optimal model that best
236 accounted for the spatio-temporal variation in schistosomiasis prevalence. Figure 3 shows its
237 superiority in predicting the schistosomiasis prevalence data, possibly because the complexity
238 of the dynamics presented in a latent process can be captured flexibly if a sufficient number of
239 parameters is available, and the CNN was trained on a massive amount of spatial data to obtain
240 this [22]. Deep neural nets, especially CNNs, contain the necessary structure to harness this
241 complexity. Furthermore, CNNs offer a global prior model for the dynamics that is both realistic
242 and computationally efficient [22].

243

244 We found that the distribution patterns of schistosomiasis infection varied over space and time
245 throughout the study period. These shifts in pattern can likely be attributed to changes in control
246 strategies implemented at different stages of schistosomiasis management, potentially leading
247 to a nonlinear dynamic process in the prevalence of the disease [15, 28]. The 10-year WBLP,
248 launched in 1992, has effectively facilitated the praziquantel chemotherapy strategy [10].
249 Figure 4 shows that the predictions indicated schistosomiasis was maintained at a relatively
250 stable and low level until 2001, after which there was a resurgence following the conclusion of
251 the WBLP. This resurgence may be due to the fact that chemotherapy measures were limited to
252 bovines and humans. Considering that over 40 species of mammals can act as potential zoonotic
253 reservoirs, these measures are insufficient to completely interrupt the life cycle of the
254 parasite [29]. Another possible explanation for the rebound is environmental and social factors,

255 such as the floods of the Yangtze River in the late 1990s, ecological changes, and population
256 movements [30, 31].

257

258 To address this issue, a comprehensive national control strategy was put into place in 2005,
259 encompassing agricultural mechanization, improved sanitation, and health education [32, 33].

260 This strategy has been effective, leading to positive changes in both environmental conditions
261 and human behaviors. Socioeconomic improvements, including better access to healthcare,
262 enhanced sanitation facilities, and changes in water-related activities, have contributed to the
263 reduction in disease transmission [34]. Furthermore, modifications in agricultural practices and
264 water management may have impacted snail habitats [35]. The success of this comprehensive
265 control strategy is evident based on the reduced number of schistosomiasis foci from 2006 to
266 2011, as shown in Figure 4. The sustained low prevalence of the disease from 2012 to 2015
267 further demonstrates the effectiveness and durability of these measures, underscoring the
268 importance of continuing with this strategy.

269

270 Our CNN-IDE model has proven its superiority over traditional models in capturing the
271 intricate spatio-temporal variations of schistosomiasis prevalence. This success is rooted in the
272 model's flexible ability to comprehend latent process complexities through an ample parameter
273 set, bolstered by extensive training on spatial data using a CNN [24]. The CNN's inherent ability
274 to process complex multilayered information enables it to accurately represent the dynamics of
275 schistosomiasis. This advantage highlights the potential of our model as a promising tool for
276 future spatio-temporal risk modeling in schistosomiasis, contributing to the advancement of
277 precision public health methodologies.

278

279 The limitations of the study need to be discussed. First, the low prevalence of schistosomiasis
280 might result from the suboptimal specificity of serological analysis and sensitivity of stool
281 examinations. It will be necessary to consider diagnostic errors in future modeling research to
282 improve prediction accuracy. Second, we only considered a limited number of environmental
283 factors and socioeconomic factors, such as household financial situations and medical

284 conditions, were not included because these covariates were not available at the village level.
285 Nevertheless, the random effect, $\eta_t(s)$, as shown in Supplementary Material Equation (2), is
286 the "residual" after discounting what the covariates explain [36]. This suggests that covariates
287 not included in our analysis are left in this "residual." Third, we obtained data on water bodies
288 in 2015, since historical and updated data on tributaries of the Yangtze River were not available.

289
290 In summary, the proposed CNN-IDE model effectively captured the complex dynamic process
291 of schistosomiasis prevalence. The high-resolution 1×1 -km grid-level maps in our study
292 facilitate the quantification of inequalities in prevalence to guide the efficient deployment of
293 resources and interventions to those with the greatest need. As researchers, policymakers, and
294 program implementors need to work together to achieve schistosomiasis elimination, our study
295 provides a precision tool, guiding them where to go next.

296 297 **Ethics approval**

298 The collection of parasitological data was part of a continuing public health investigation
299 determined by the National Health and Family Planning Commission. Hence, this study was
300 exempt from institutional review board assessment.

301 302 **Competing Interests**

303 We declare that we have no conflicts of interest.

304 305 **Consent for publication**

306 Not applicable.

307 308 **Availability of data and materials**

309 The datasets used and analyzed during the current study are available from the corresponding
310 author on reasonable request and from a website repository (<http://cdc.cma.gov.cn/home.do>,
311 <http://ladsweb.nascom.nasa.gov>, <http://worldwildlife.org>).

312

313 **Funding**

314 This work is primarily being funded by the National Natural Science Foundation of China
315 (81773487,81973102).

316

317 **Acknowledgements**

318 We would like to express gratitude to all the people who participated in data collection, as well
319 as to our teachers for guiding and revising the paper.

320

321

322 **References**

- 323 1. King CH, Dickman K, Tisch DJ. Reassessment of the cost of chronic helminthic infection: a meta-analysis of
324 disability-related outcomes in endemic schistosomiasis. *Lancet* 2005; 365:1561-1569.
- 325 2. WHO. Control of Neglected Tropical Diseases. World Health Organization; 2021 [cited 2022 Apr 17]. Available
326 from:<https://www.who.int/health-topics/schistosomiasis>.
- 327 3. Global, regional, and national incidence, prevalence, and years lived with disability for 354 diseases and injuries
328 for 195 countries and territories, 1990-2017: a systematic analysis for the Global Burden of Disease Study 2017.
329 *Lancet* 2018; 392:1789-1858.
- 330 4. Gordon CA, Kurscheid J, Williams GM, Clements ACA, Li Y, Zhou XN, et al. Asian Schistosomiasis: Current
331 Status and Prospects for Control Leading to Elimination. *Trop Med Infect Dis* 2019; 4
- 332 5. Shou-Pai M, Bao-Ruo S. Schistosomiasis control in the People's Republic of China. *The American journal of*
333 *tropical medicine and hygiene* 1982; 31:92-99.
- 334 6. Zhang LJ, Xu ZM, Yang F, Dang H, Li YL, Lü S, et al. Endemic status of schistosomiasis in People's Republic
335 of China in 2020. *Zhongguo Xue Xi Chong Bing Fang Zhi Za Zhi* 2021; 33:225-233.
- 336 7. Heuvelink GB, Griffith DA. Space-Time Geostatistics for Geography: A Case Study of Radiation Monitoring
337 Across Parts of Germany. *Geographical analysis* 2010; 42:161-179.
- 338 8. Xianyi C, Liying W, Jiming C, Xiaonong Z, Jiang Z, Jiagang G, et al. Schistosomiasis control in China: the
339 impact of a 10-year World Bank Loan Project (1992-2001). *Bull World Health Organ* 2005; 83:43-48.
- 340 9. Collins C, Xu J, Tang S. Schistosomiasis control and the health system in P.R. China. *Infect Dis Poverty* 2012;
341 1:8.
- 342 10. Liu R, Dong HF, Jiang MS. The new national integrated strategy emphasizing infection sources control for
343 schistosomiasis control in China has made remarkable achievements. *Parasitol Res* 2013; 112:1483-1491.
- 344 11. Hu Y, Gao J, Chi M, Luo C, Lynn H, Sun L, et al. Spatio-temporal patterns of schistosomiasis japonica in lake
345 and marshland areas in China: the effect of snail habitats. *Am J Trop Med Hyg* 2014; 91:547-554.
- 346 12. Hu Y, Li R, Bergquist R, Lynn H, Gao F, Wang Q, et al. Spatio-temporal transmission and environmental
347 determinants of Schistosomiasis Japonica in Anhui Province, China. *PLoS Negl Trop Dis* 2015; 9:e0003470.
- 348 13. Hu Y, Zhang Z, Chen Y, Wang Z, Gao J, Tao B, et al. Spatial pattern of schistosomiasis in Xingzi, Jiangxi
349 Province, China: the effects of environmental factors. *Parasit Vectors* 2013; 6:214.
- 350 14. Zhang ZJ, Carpenter TE, Lynn HS, Chen Y, Bivand R, Clark AB, et al. Location of active transmission sites of
351 *Schistosoma japonicum* in lake and marshland regions in China. *Parasitology* 2009; 136:737-746.

- 352 15. Hu Y, Bergquist R, Chen Y, Ke Y, Dai J, He Z, et al. Dynamic evolution of schistosomiasis distribution under
353 different control strategies: Results from surveillance covering 1991-2014 in Guichi, China. *PLoS Negl Trop*
354 *Dis* 2021; 15:e0008976.
- 355 16. Miyashita K, Itoh H, Nakao K. [Idiopathic hyperaldosteronism (IHA)]. *Nihon Rinsho* 2006; Suppl 1:624-627.
- 356 17. Yu JM, de Vlas SJ, Jiang QW, Gryseels B. Comparison of the Kato-Katz technique, hatching test and indirect
357 hemagglutination assay (IHA) for the diagnosis of *Schistosoma japonicum* infection in China. *Parasitol Int*
358 2007; 56:45-49.
- 359 18. Su Q, Bergquist R, Ke Y, Dai J, He Z, Gao F, et al. A comparison of modelling the spatio-temporal pattern of
360 disease: a case study of schistosomiasis japonica in Anhui Province, China. *Trans R Soc Trop Med Hyg* 2021;
- 361 19. Box GE, Cox DR. An analysis of transformations. *J R Stat Soc: Series B (Methodological)* 1964; 26:211-243.
- 362 20. Diggle PJ, Tawn JA, Moyeed RA. Model-based geostatistics. *J R Stat Soc: Series C (Applied Statistics)* 1998;
363 47:299-350.
- 364 21. Hu Y, Xiong C-L, Zhang Z-J, Bergquist R, Wang Z-L, Gao J, et al. Comparison of data-fitting models for
365 schistosomiasis: a case study in Xingzi, China. *Geospatial health* 2013:125-132.
- 366 22. Mangion AZ, Wikle CK. Deep Integro-Difference Equation Models for Spatio-Temporal Forecasting. *CoRR*,
367 vol. abs/1910.13524 2019;
- 368 23. Wikle CK, Zammit-Mangion A, Cressie N. *Spatio-temporal statistics with R*: CRC Press; 2019, p. 258-266.
- 369 24. Zhu HR, Liu L, Zhou XN, Yang GJ. Ecological Model to Predict Potential Habitats of *Oncomelania hupensis*,
370 the Intermediate Host of *Schistosoma japonicum* in the Mountainous Regions, China. *PLoS Negl Trop Dis*
371 2015; 9:e0004028.
- 372 25. Ajakaye OG, Adedeji OI, Ajayi PO. Modeling the risk of transmission of schistosomiasis in Akure North Local
373 Government Area of Ondo State, Nigeria using satellite derived environmental data. *PLoS Negl Trop Dis* 2017;
374 11:e0005733.
- 375 26. Gao F, Ward MP, Wang Y, Zhang Z, Hu Y. Implications from assessing environmental effects on spatio-
376 temporal pattern of schistosomiasis in the Yangtze Basin, China. *Geospat Health* 2018; 13
- 377 27. Pflüger W. Experimental epidemiology of schistosomiasis. *Zeitschrift für Parasitenkunde* 1980; 63:159-169.
- 378 28. Hu Y, Xiong C, Zhang Z, Luo C, Ward M, Gao J, et al. Dynamics of spatial clustering of schistosomiasis in
379 the Yangtze River Valley at the end of and following the World Bank Loan Project. *Parasitol Int* 2014; 63:500-
380 505.
- 381 29. Zhou YB, Liang S, Jiang QW. Factors impacting on progress towards elimination of transmission of
382 schistosomiasis japonica in China. *Parasit Vectors* 2012; 5:275.
- 383 30. Zhou XN, Guo JG, Wu XH, Jiang QW, Zheng J, Dang H, et al. Epidemiology of schistosomiasis in the People's
384 Republic of China, 2004. *Emerg Infect Dis* 2007; 13:1470-1476.
- 385 31. Wang L, Utzinger J, Zhou XN. Schistosomiasis control: experiences and lessons from China. *Lancet* 2008;
386 372:1793-1795.
- 387 32. Wang LD, Guo JG, Wu XH, Chen HG, Wang TP, Zhu SP, et al. China's new strategy to block *Schistosoma*
388 *japonicum* transmission: experiences and impact beyond schistosomiasis. *Trop Med Int Health* 2009; 14:1475-
389 1483.
- 390 33. Wang LD, Chen HG, Guo JG, Zeng XJ, Hong XL, Xiong JJ, et al. A strategy to control transmission of
391 *Schistosoma japonicum* in China. *N Engl J Med* 2009; 360:121-128.
- 392 34. Ben-Jiao H, Hong-Ling X, Sheng-Ming L, Zheng-Yuan Z, Yi-Biao Z, Zhi-Hong L, et al. [Measures and
393 achievements of schistosomiasis control in the Yangtze River Basin]. *Zhongguo Xue Xi Chong Bing Fang Zhi*
394 *Za Zhi* 2018; 30:592-595.
- 395 35. Guo S, Dang H, Li Y, Zhang L, Yang F, He J, et al. Sentinel Surveillance of Schistosomiasis - China, 2021.

396 China CDC Wkly 2023; 5:278-282.

397 36. Wikle CK, Zammit-Mangion A, Cressie N. Spatio-temporal statistics with R: CRC Press; 2019, p. 210-226.

398

Epub ahead of print

399 **Figure legend**

400

401 **Figure 1. Endemic areas of schistosomiasis in Anhui Province, China.** Anhui Province is
402 located in the lower reaches of the Yangtze River in eastern China.

403

404 **Figure 2. Box plot for the observed prevalence of schistosomiasis in sample villages in**
405 **Anhui, China, from 1997 to 2015.** The blue line represents the average annual prevalence, and
406 the red points are the median annual prevalence. The boxes denote minimum, median,
407 maximum, and interquartile ranges.

408

409 **Figure 3. Average mean squared prediction error (MSPE) (top) and continuous ranked**
410 **probability score (CRPS) (bottom) of the CNN-IDE predictions (red), the IDE predictions**
411 **(green) and the ST Kriging predictions (blue) as a function of time. CNN, convolutional**
412 **neural network; IDE, integro-difference equation.**

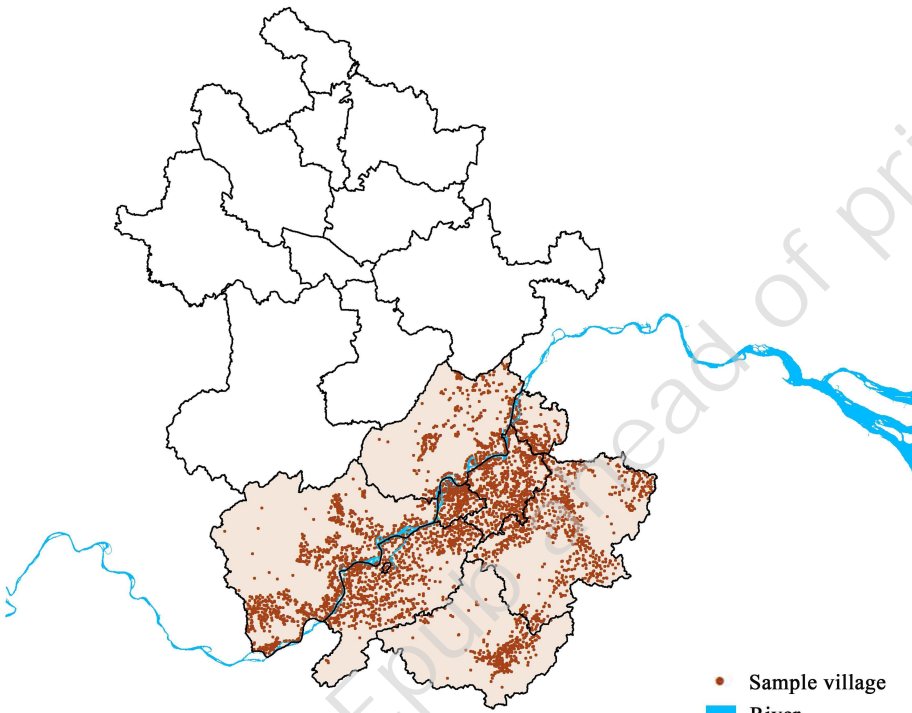
413

414 **Figure 4. Plot for the annual prevalence of schistosomiasis predicted from 1997 to 2015 in**
415 **Anhui Province, China.**

416

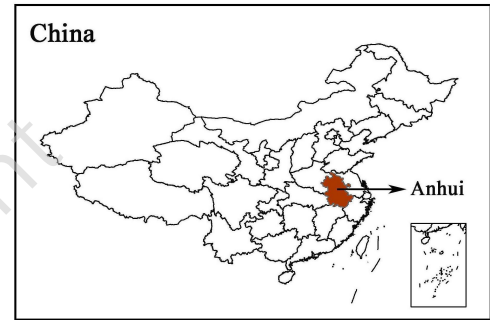
417 **Figure 5. Plot for the annual standard error of the predicted prevalence of schistosomiasis**
418 **from 1997 to 2015 in Anhui Province, China.**

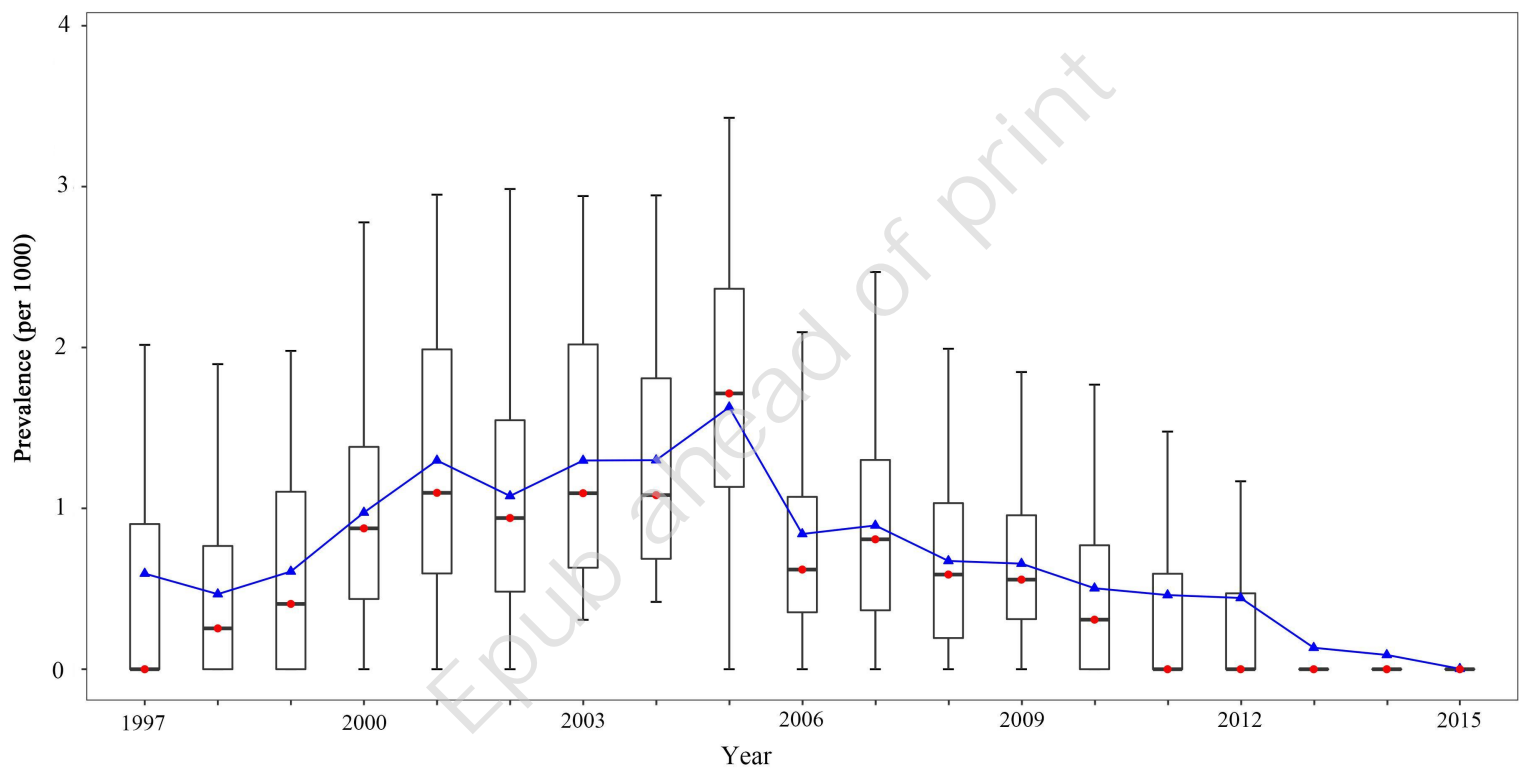
419

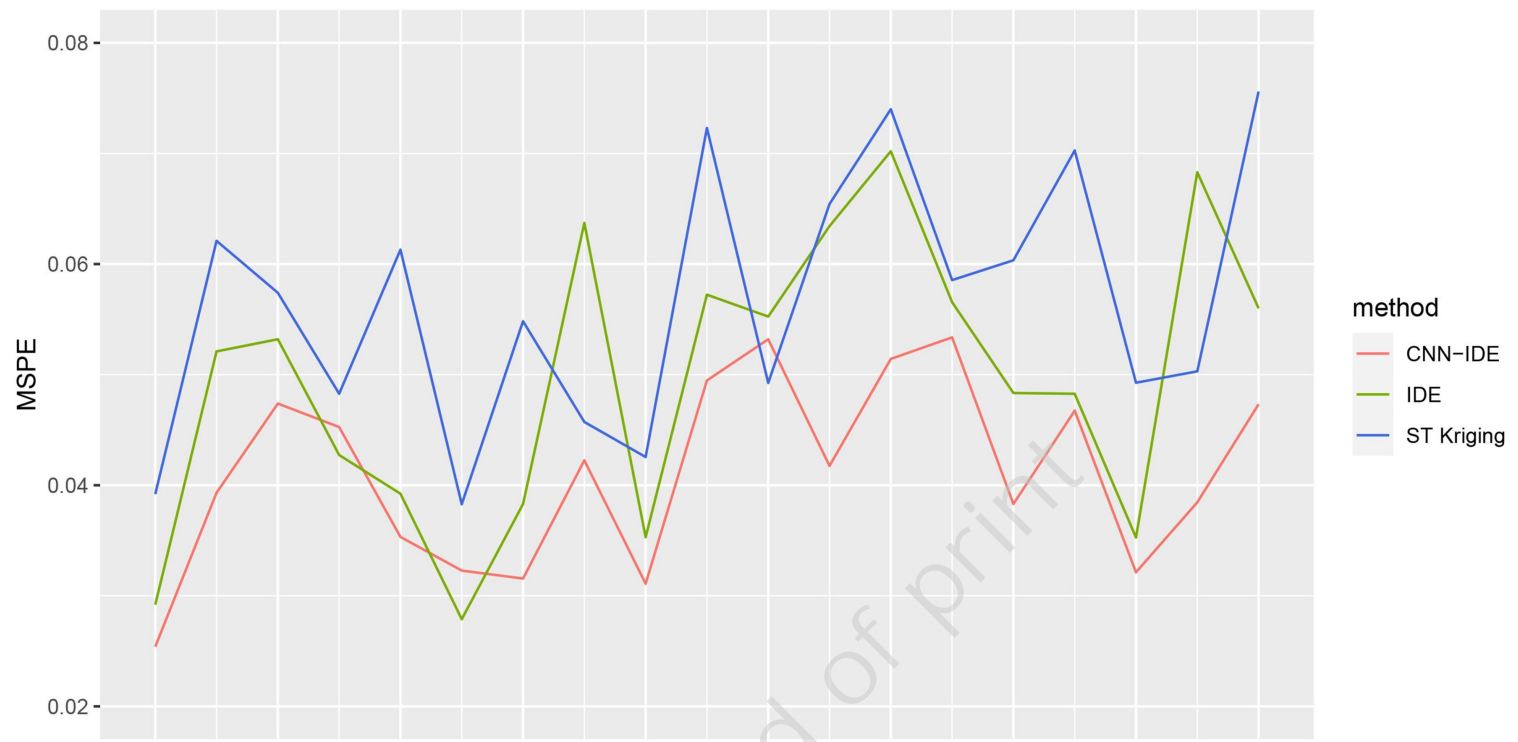


- Sample village
- River
- Endemic area

0 50 100 200 km





a**b**